HIM

Henbest &
Couper “Guide
to the Galaxy”

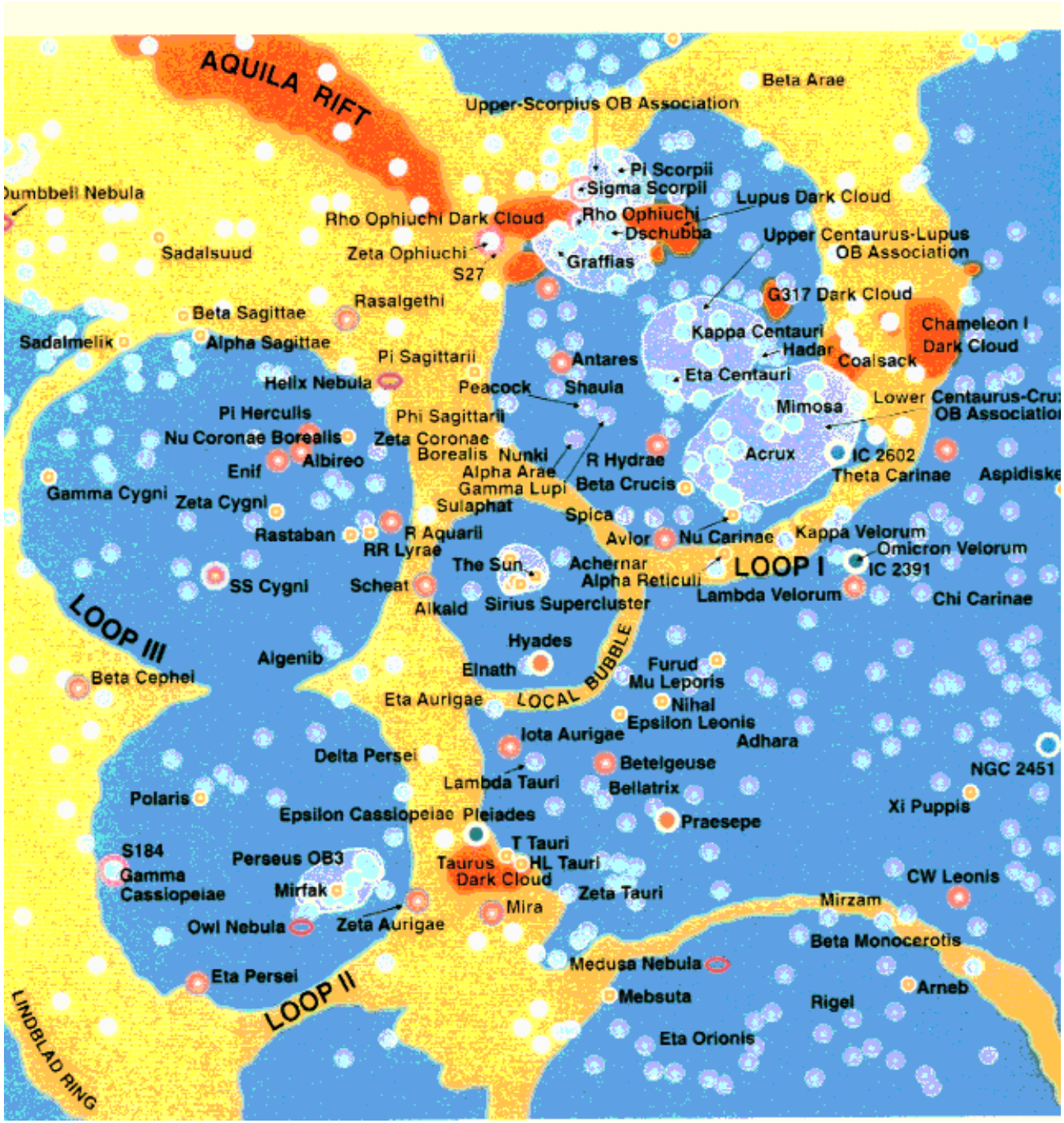

Galactic fountain

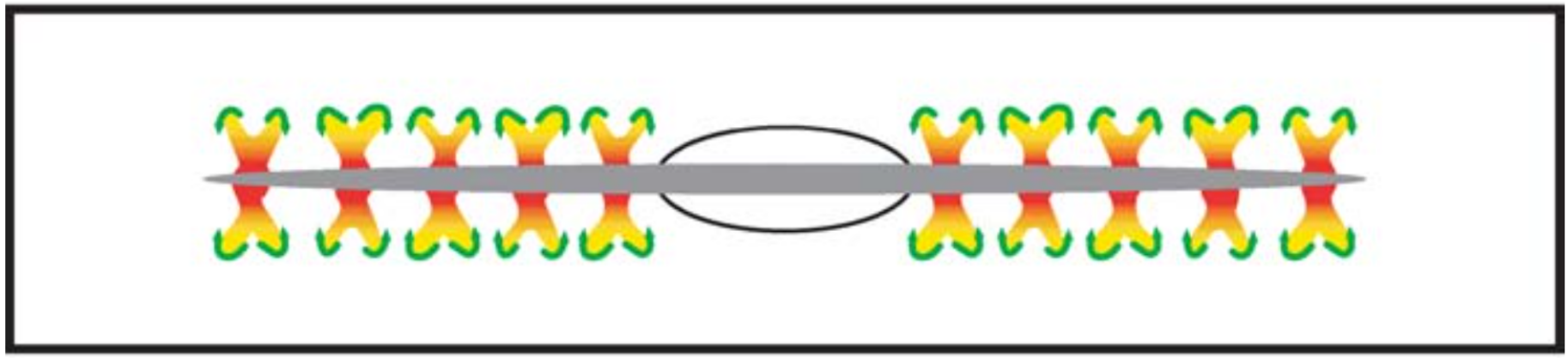

Cox 2005, ARAA

ROSAT (Snowden+ 1997)

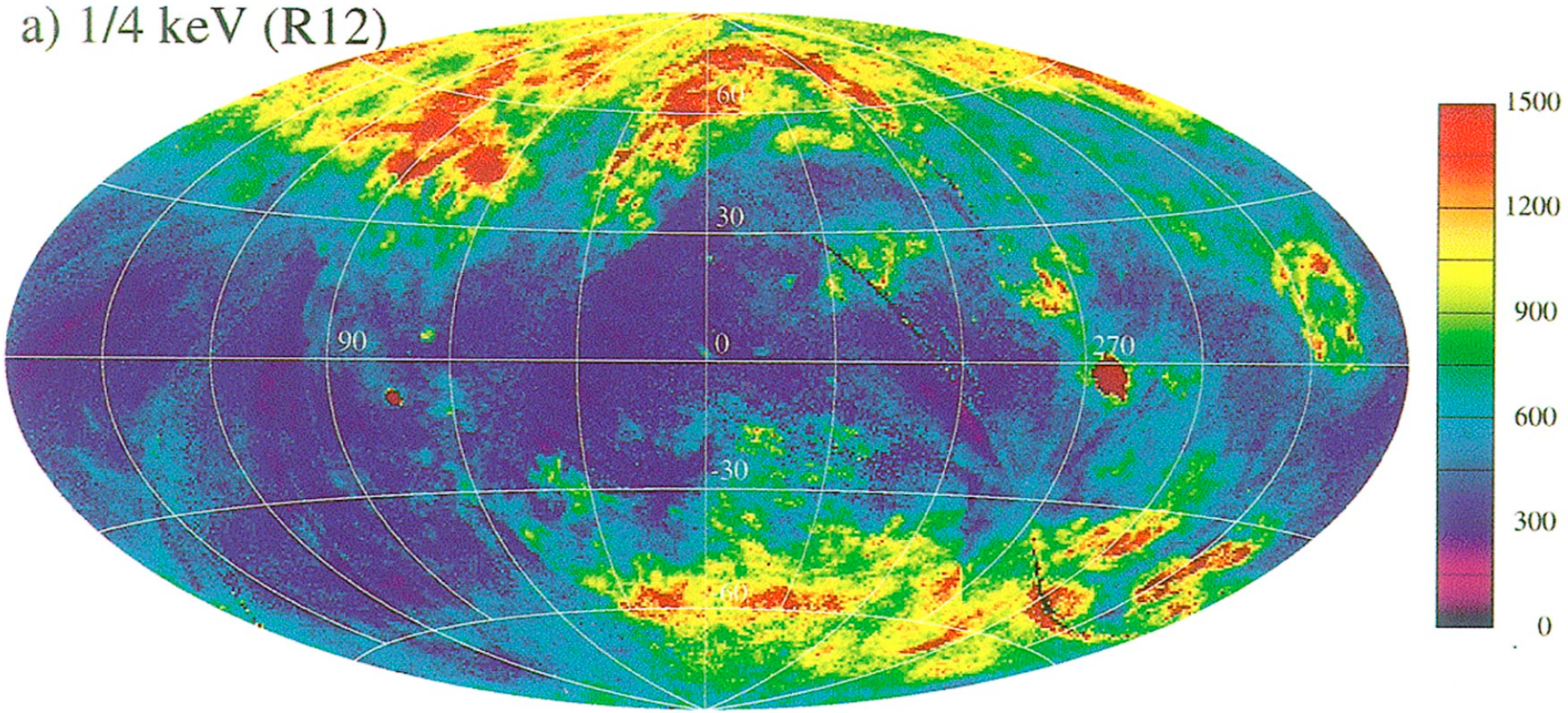

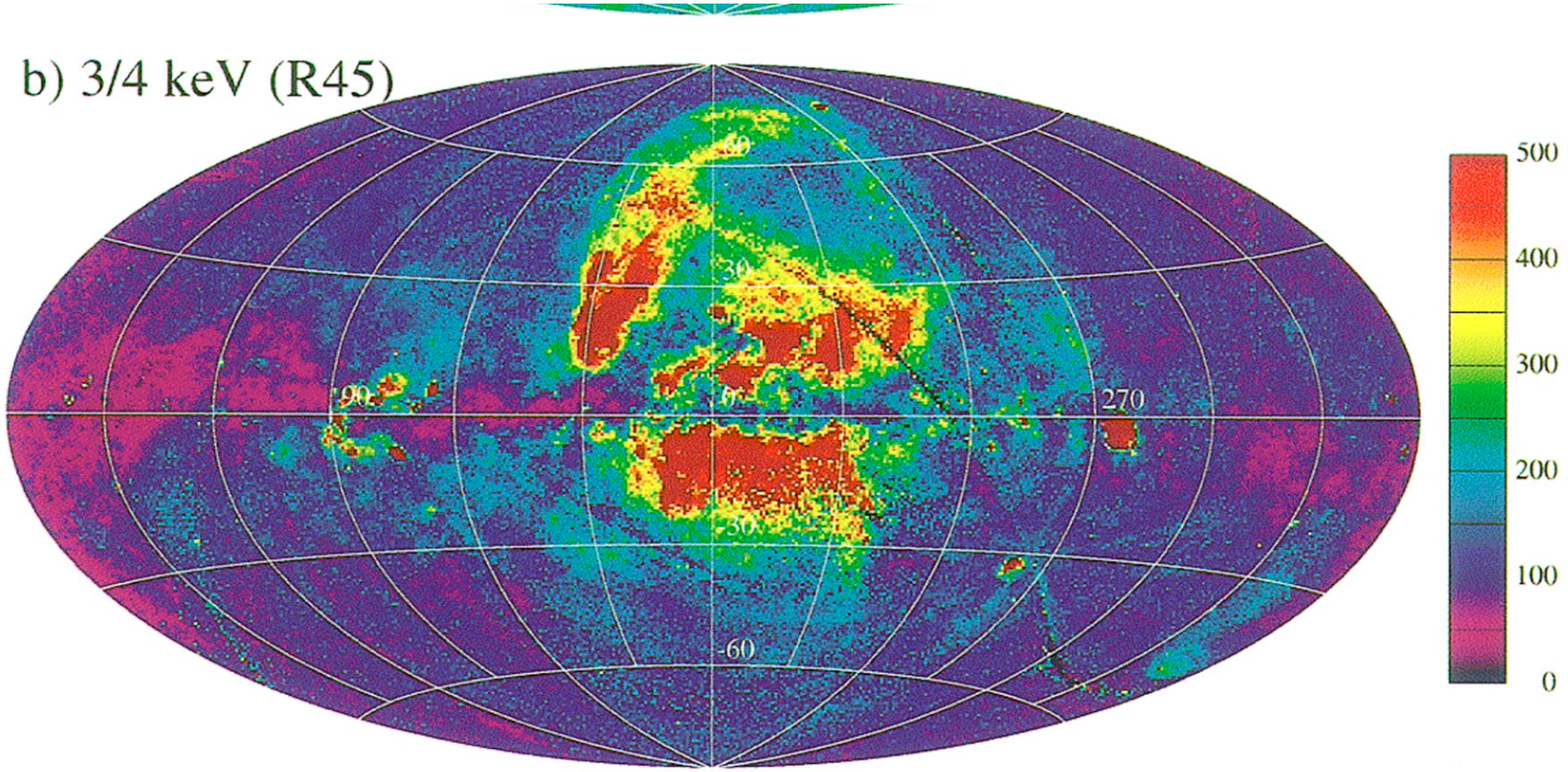
b) 3/4 keV (R45)
60
30
0
-30
-60
90
270
500
400
300
200
100
0

c) 1.5 keV (R67)

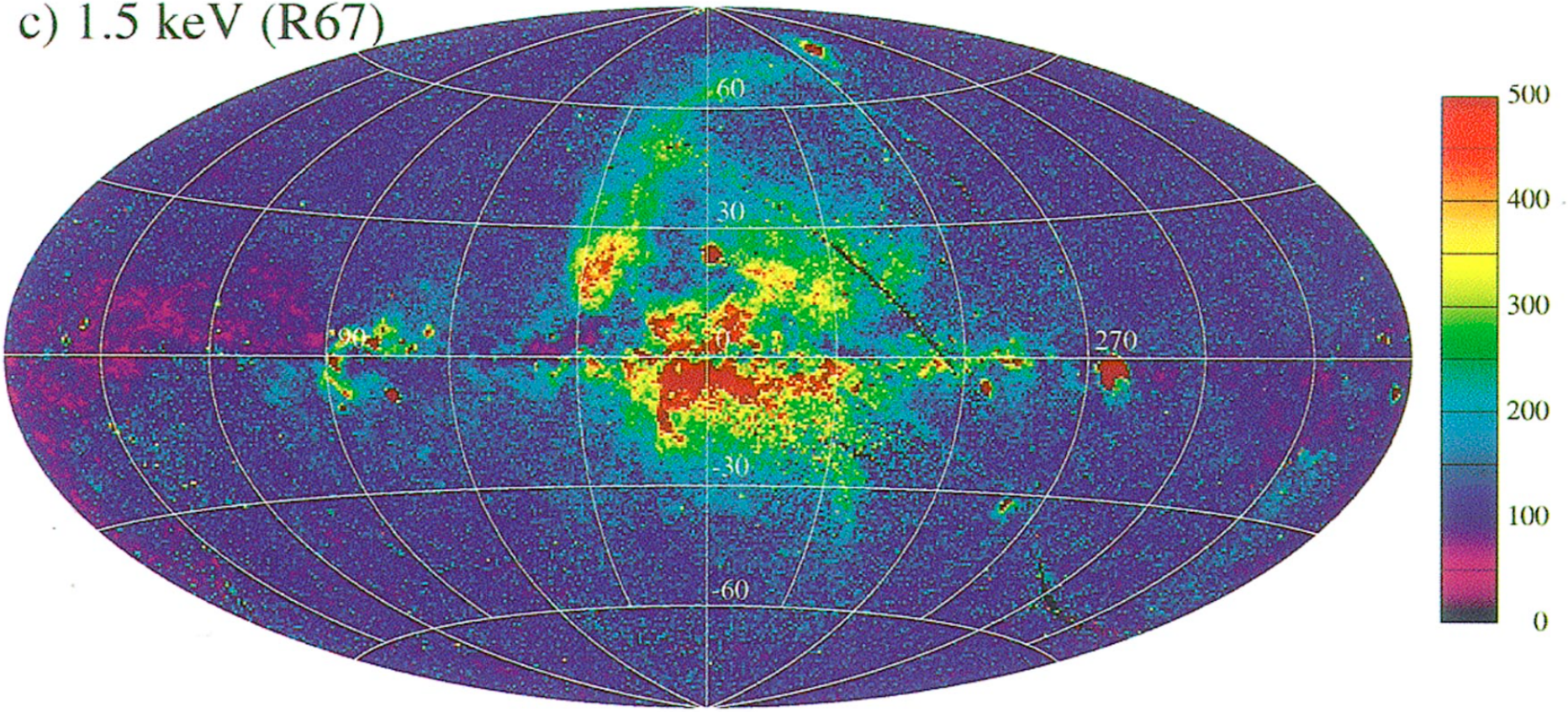

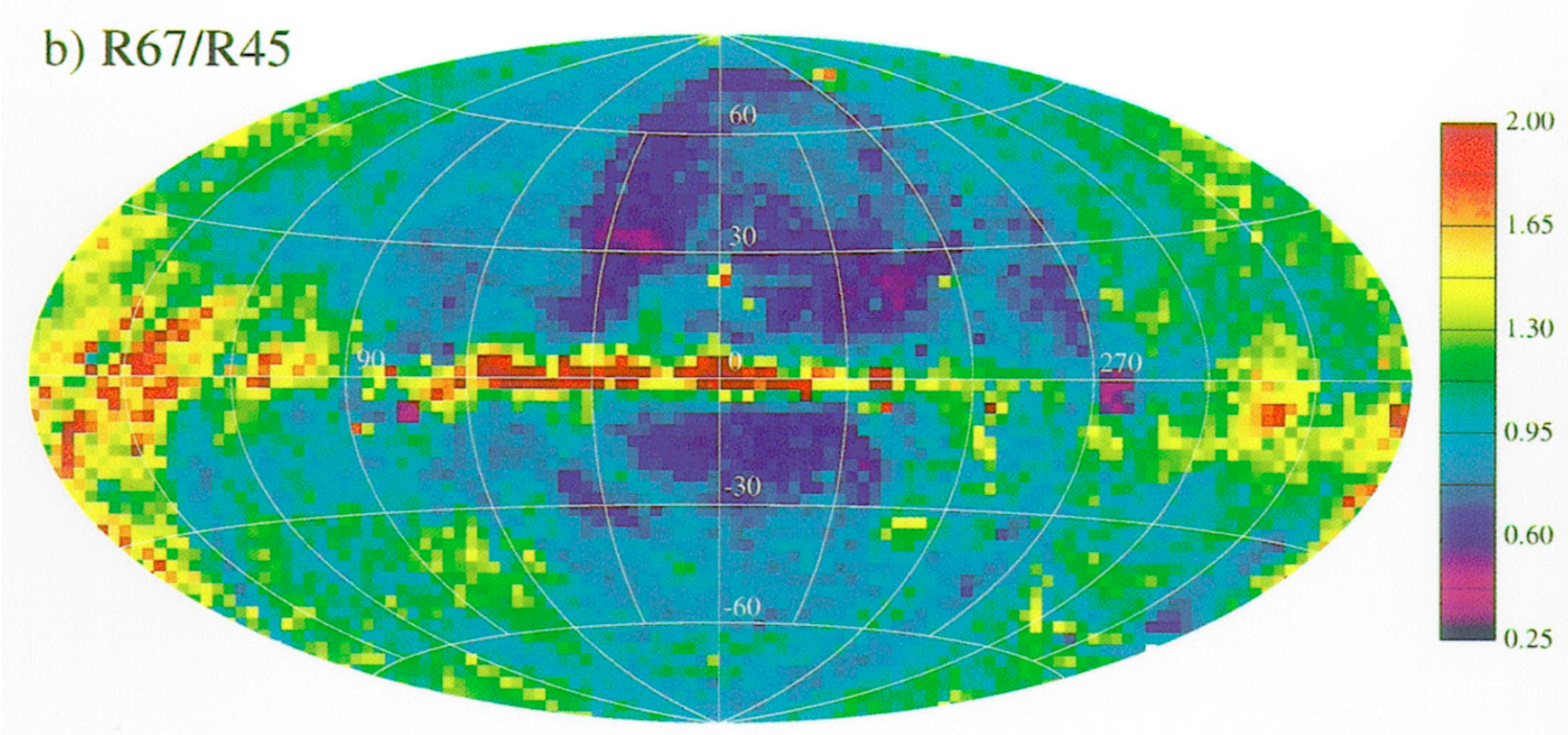
b) R67/R45
60
30
90
0
270
-30
-60
2.00
1.65
1.30
0.95
0.60
0.25

Heiles, Haffner, & Reynolds 1999 “The Eridanus Superbubble inits Multiwavelength Glory”

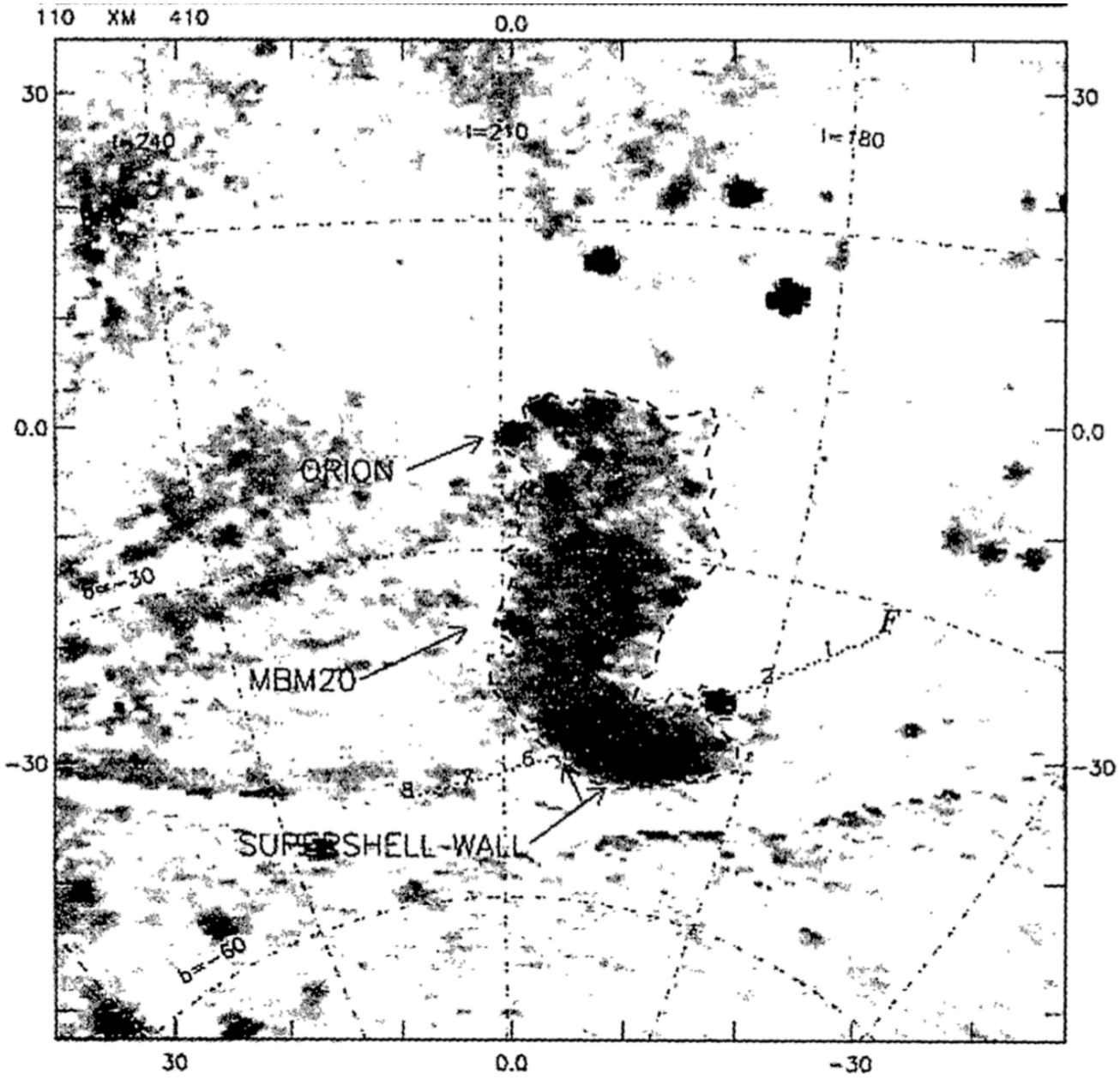

Figure 1. XM-band emission ($\frac{3}{4}$ keV, from gas at $T \sim 2\times10^6$ K) from Snowden et al (1995b). The grey scale is calibrated by the colorbar on

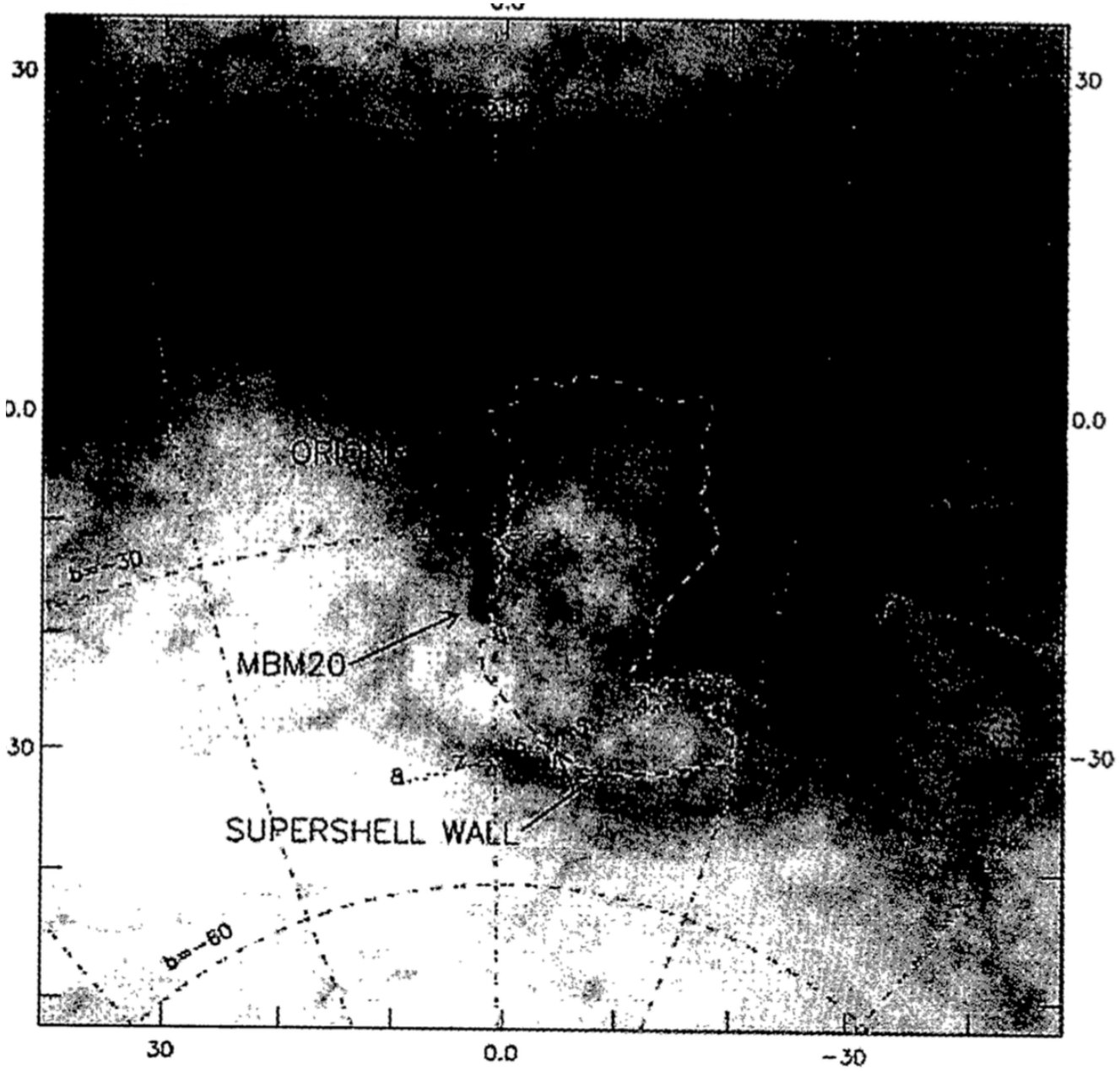

Figure 3. 100 μm emission from IRAS. To obtain $N(HI)_{20}$ in regions of low column density, multiply by about 1.5. See caption for Figure 1.

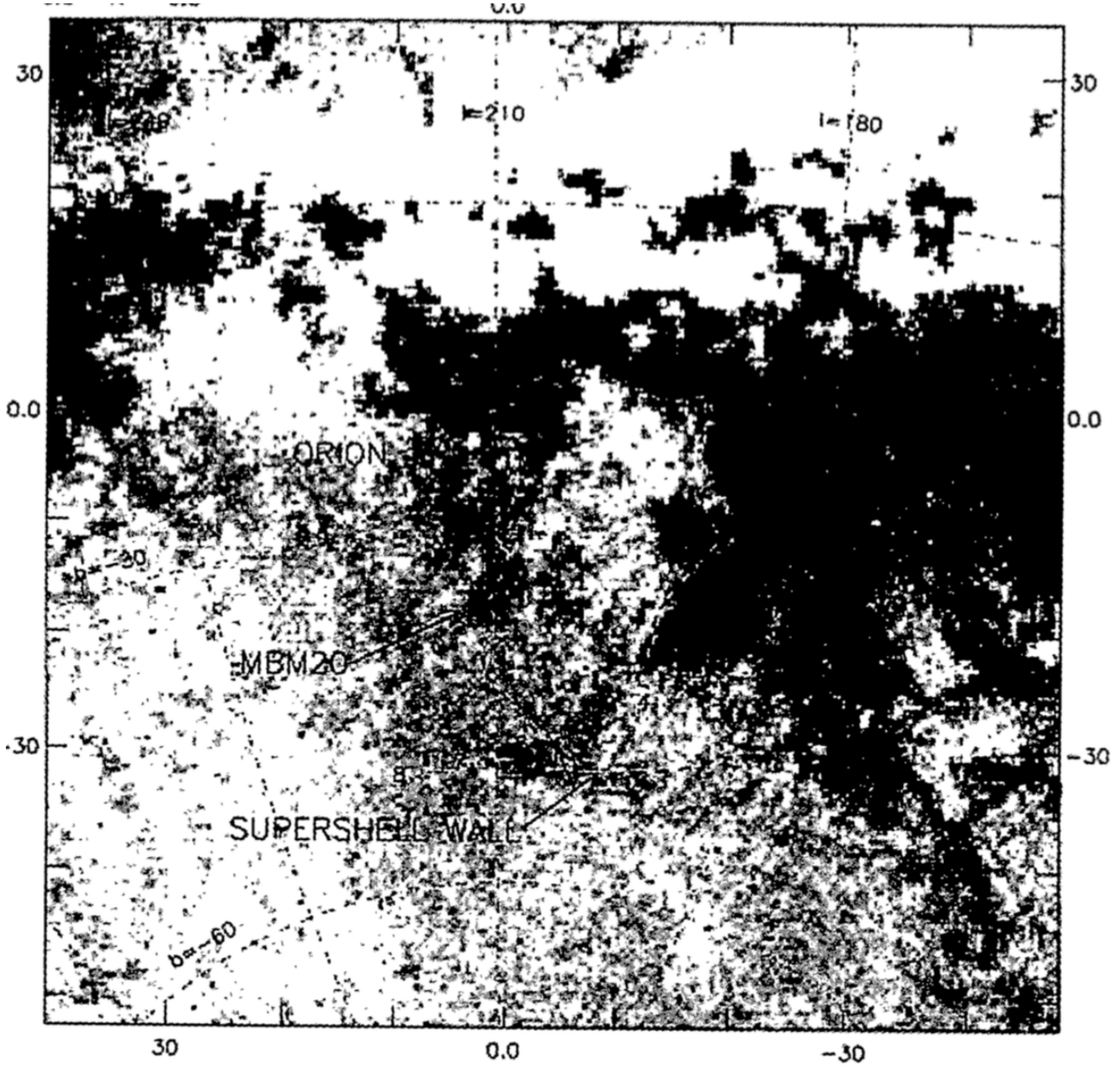

Figure 5. R, the residual temperature-corrected IR emission from equation (3), indicating H_2. The grey scale is calibrated by the colorbar

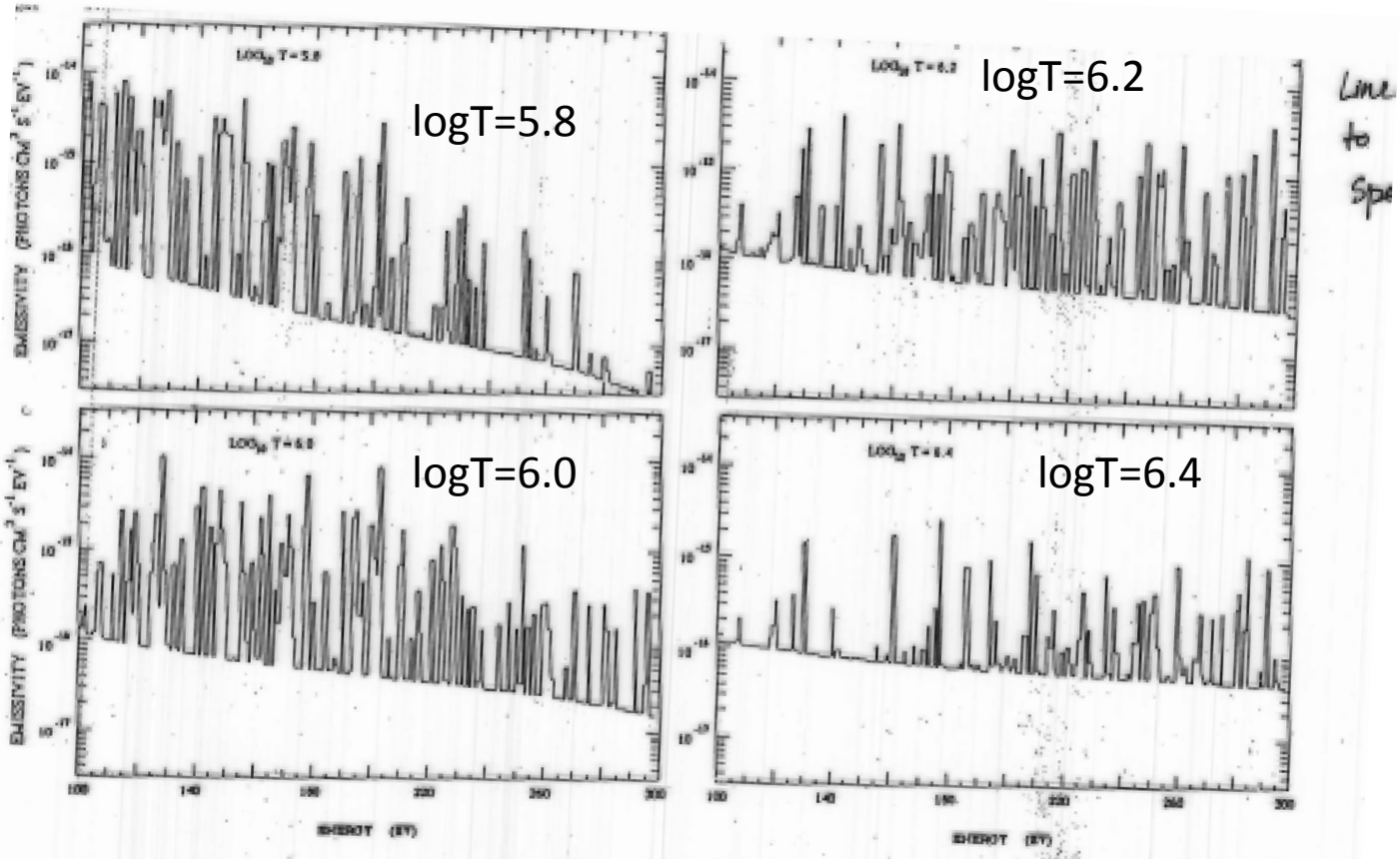

Figure 3. The emissivity ε_υ(photons $cm^3 s^{-1} eV^{-1}$) of a hot optically thin plasma of solar abundances at logT = 5.8, 6.0, 6.2 and 6.4 according to recent unpublished calculations of Raymond which represent an update to the work of Raymond and Smith (1977). The plasma produces a combination of line and continuum emission. The energy range shown (100 to 300 eV) covers the B(130-188 eV) and C(160-284eV) diffuse X-ray bands. The diagram was kindly provided by S.Snowden.

Raymond, Cox, & Smith 1976 (see also Raymond & Smith 1977)

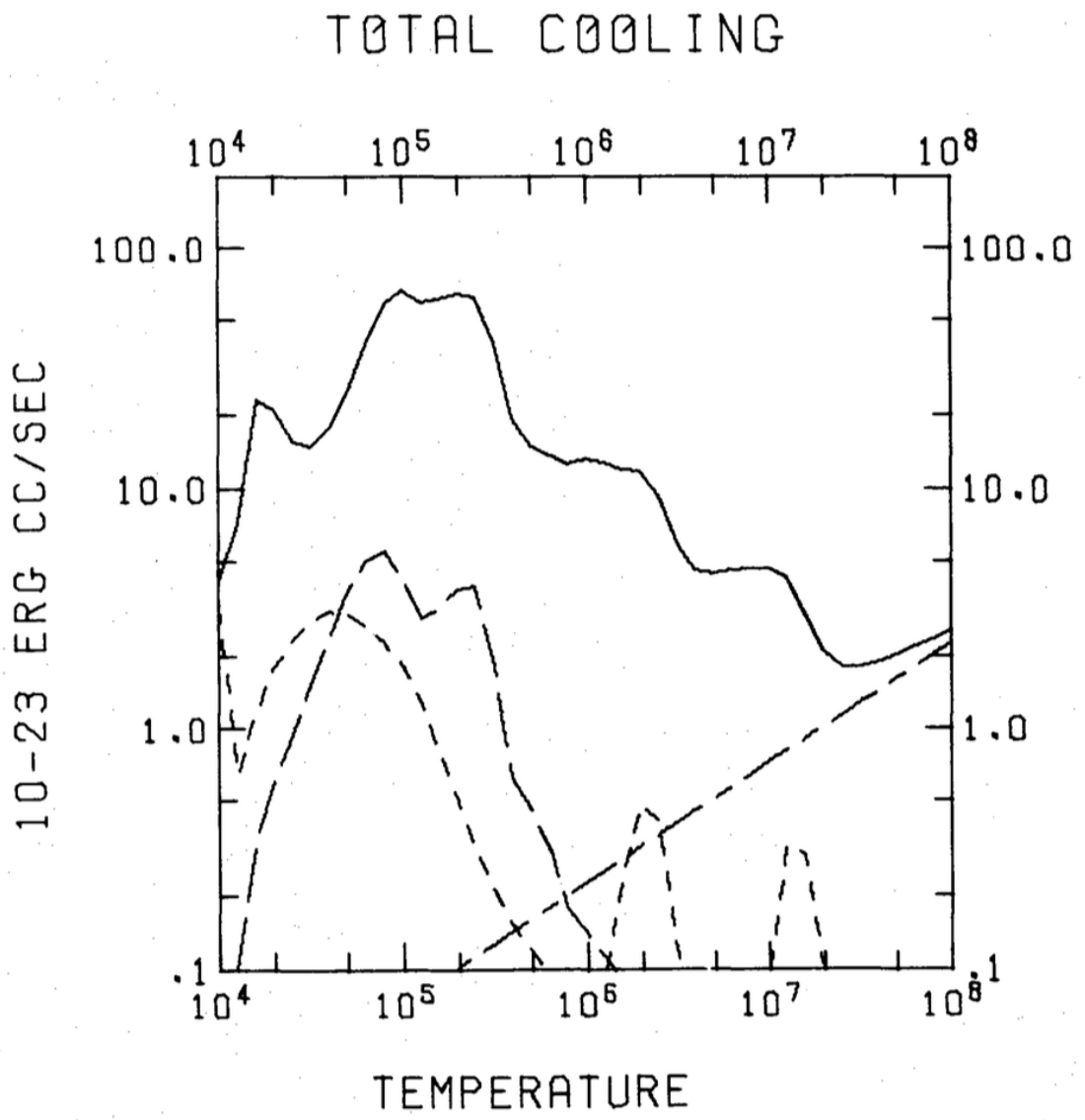

FIG. 1.—Total cooling coefficient (————), forbidden line cooling (– – – – – – –), semiforbidden line cooling (— — —), and bremsstrahlung (— — — — —).

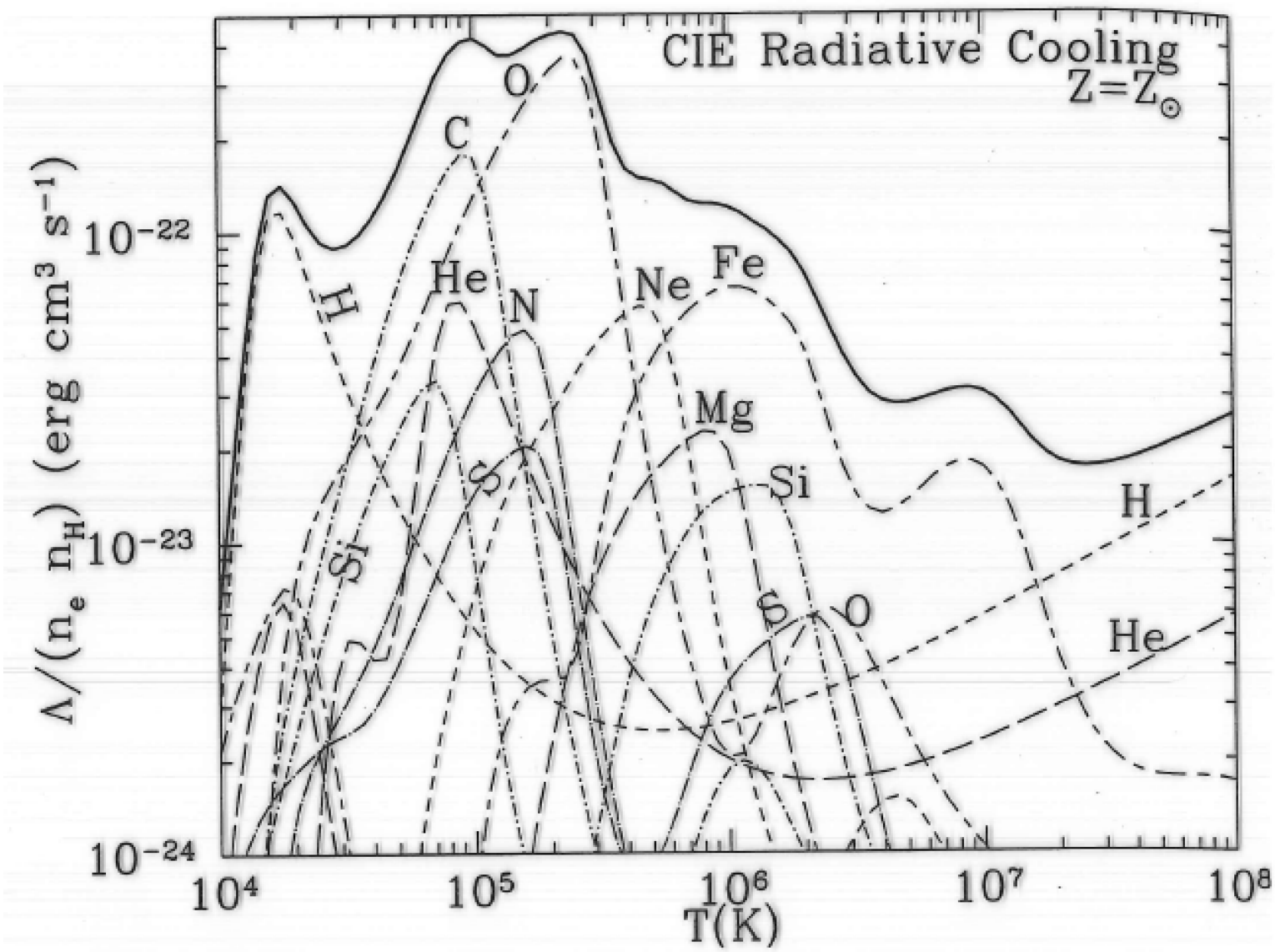

Figure 34.3 Solid line: radiative cooling function $\Lambda/n_e n_{\rm H}$ from Fig. 34.1, with contributions from selected elements shown.

Southerland & Dopita 1993

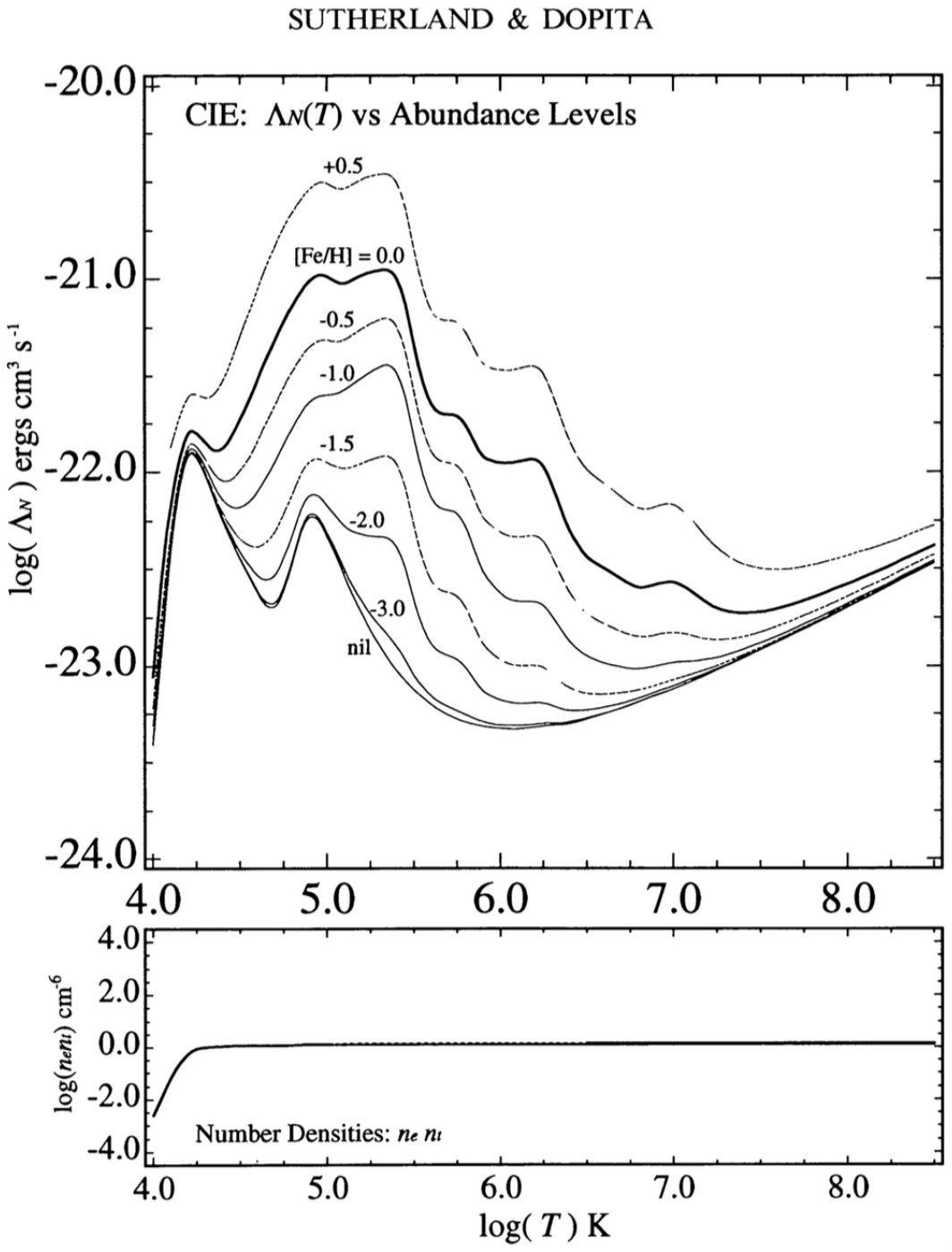

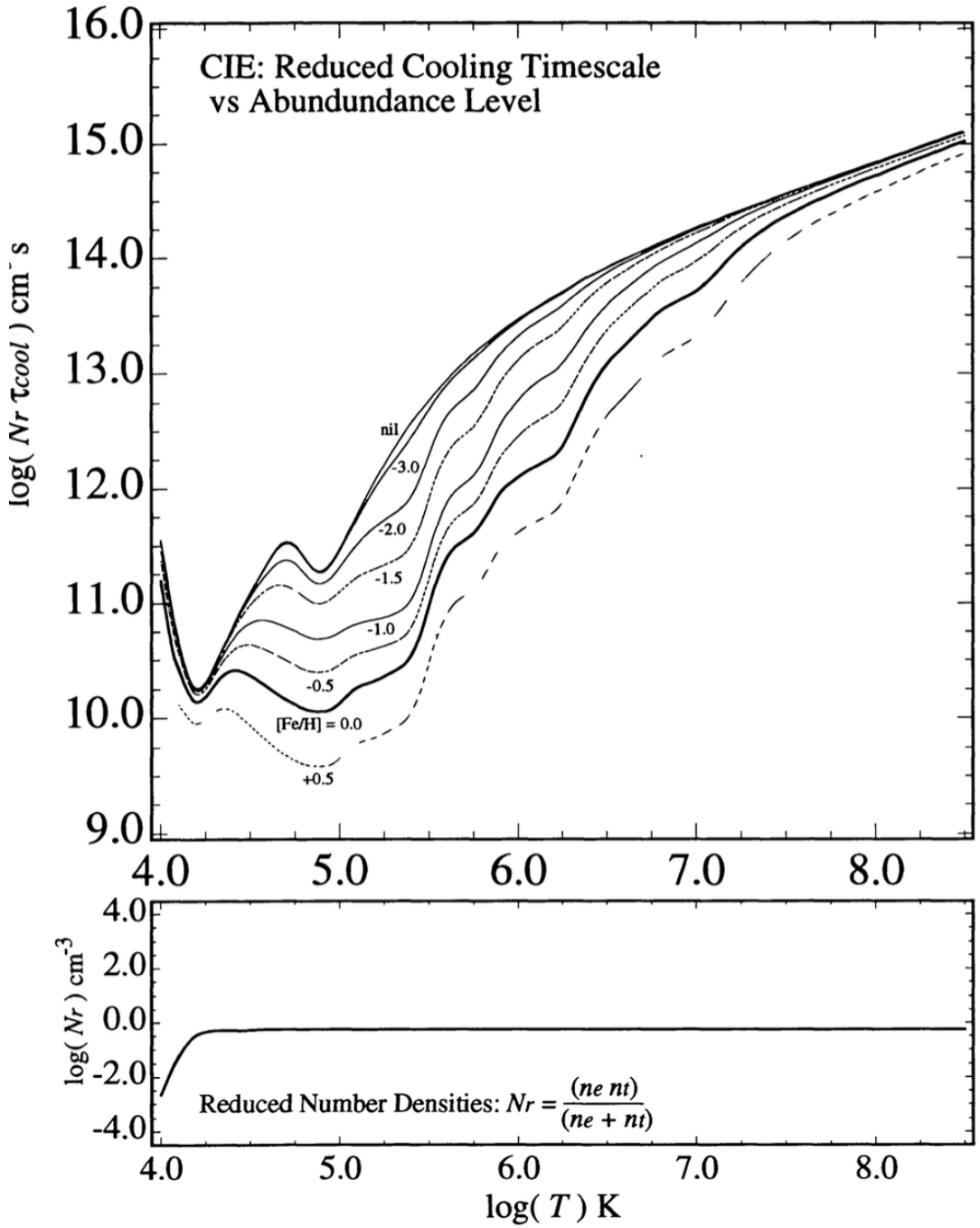
CIE: Reduced Cooling Timescale
vs Abundundance Level
log(Nr τcool) cm s
16.0
15.0
14.0
13.0
12.0
11.0
10.0
9.0
nil
-3.0
-2.0
-1.5
-1.0
-0.5
[Fe/H] = 0.0
+0.5
4.0
5.0
6.0
7.0
8.0
log(Nr) cm-3
4.0
2.0
0.0
-2.0
-4.0
Reduced Number Densities: Nr = (ne nt) / (ne + nt)
log(T) K

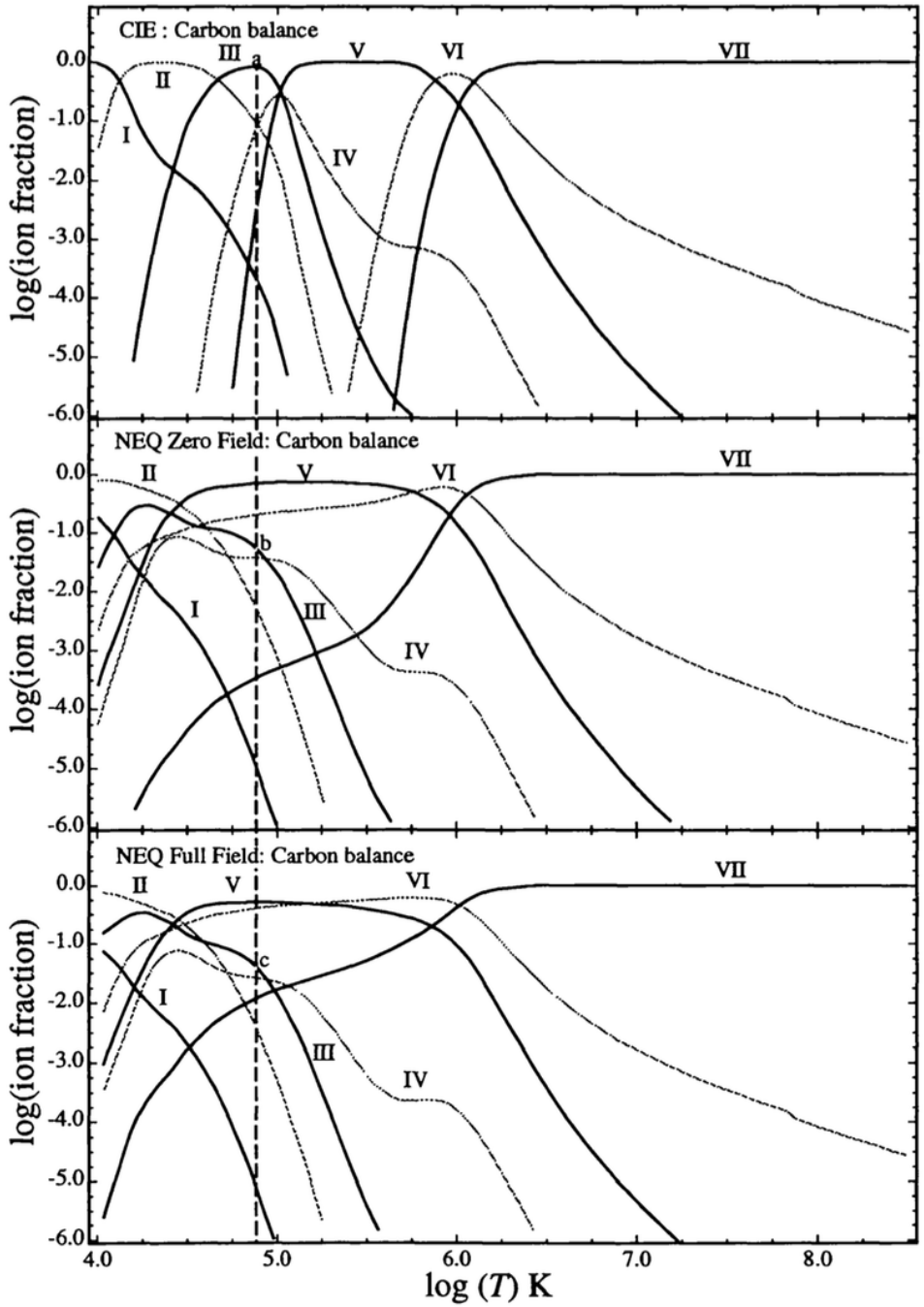

FIG. 16.—Carbon ionization balance for CIE and NEQ cases. The

Jenkins 1978

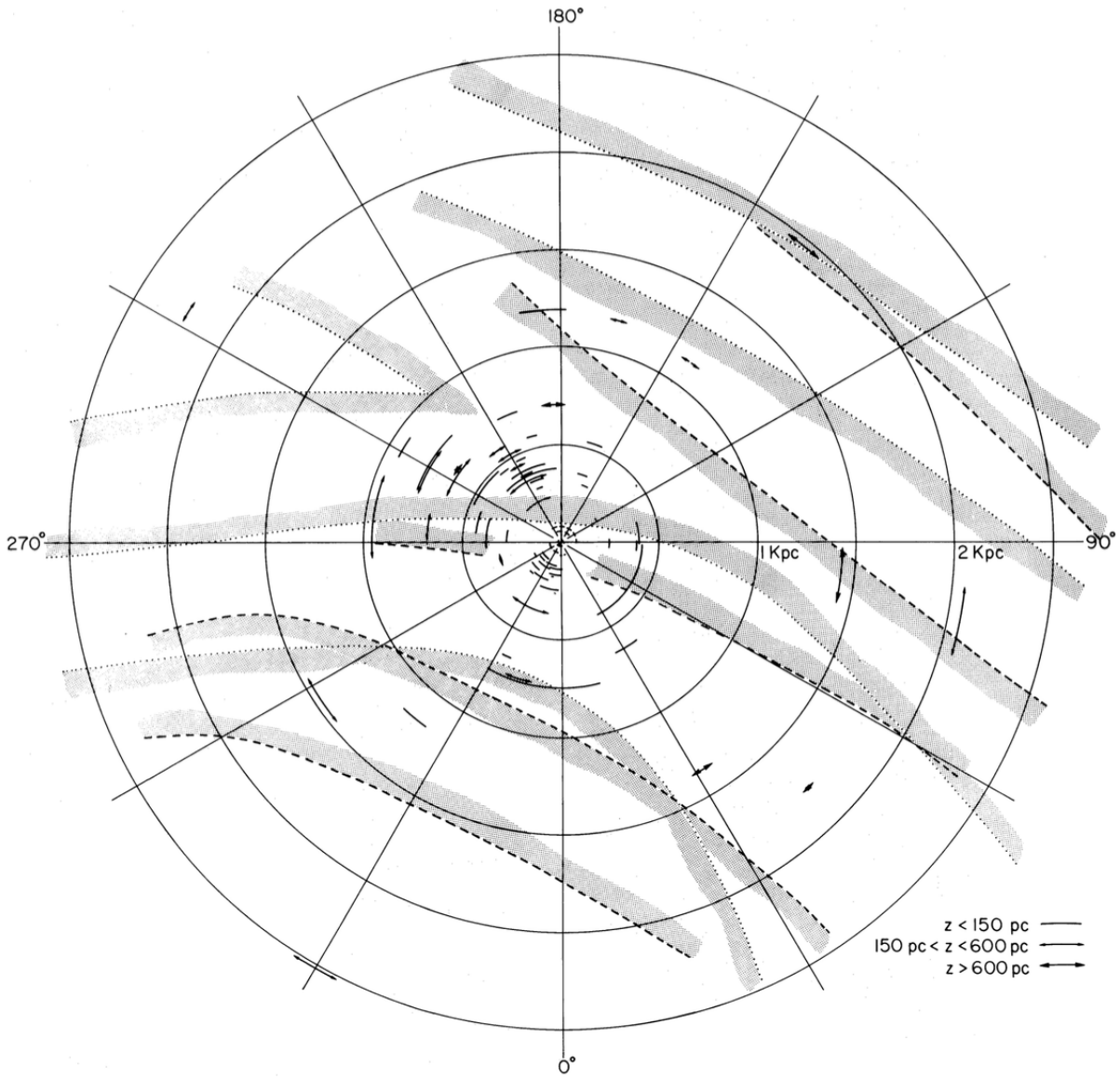

FIG. 4.—Plan view of the local region of our Galaxy centered on the Sun. Each observation is shown as an arc centered on the projection of the star's position on the galactic plane. The angle subtended by an arc is equal to the average density along the line of sight to the star, where 1° is equivalent to 1.62×10^{-9} cm^{-3}. The length of an arc indicates the column density which would be obtained if the O VI space densities along an inclined path to the star were projected onto the plane. Broken arcs show upper-limit values for stars with no absorption detected. Stars at some distance from the plane have arcs with arrows (see legend) indicating that the measurements probably understate the densities along the plane, owing to the apparent systematic decrease in O VI observed for large z (see § IV*a* of Paper II). Local galactic structure from two sources is shown for *boundaries* of the three local arms (*dotted lines:* Walborn [1973]; *dashed lines:* author's interpretation of structure seen in Schmidt-Kaler [1964]). Each boundary has shading which indicates the direction of an arm's interior.

Dwek 1987

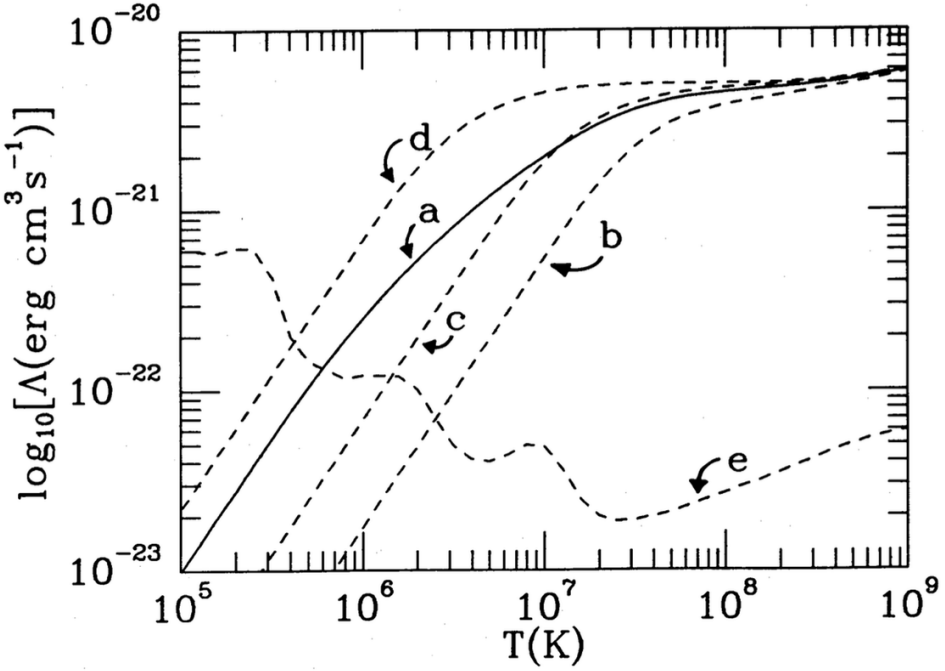

FIG. 4.—The cooling function of the gas via gas-grain collisions, $\Lambda_d(T)$, plotted as a function of gas temperature T, for: the "extended" MRN interstellar dust model (*curve a*); a silicate-graphite mixture of 0.4 μm dust particles (*curve b*); a silicate-graphite mixture of 0.1 μm dust particles (*curve c*); and a silicate-graphite mixture of 0.01 μm dust particles (*curve d*). Curve (*e*) is the cooling function of the gas, $\Lambda(T)$, due to atomic processes (Raymond, Cox, and Smith 1976) and is included in the figure for sake of comparison.